



Transactions of the 13th International Conference on Structural Mechanics in Reactor Technology (SMiRT 13), Escola de Engenharia - Universidade Federal do Rio Grande do Sul, Porto Alegre, Brazil, August 13-18, 1995

Effects of high damping rubber bearing on seismic response of superstructure in base isolated system

Yoo, B.¹, Lee, J.H.¹, Koo, G.H.¹, Kim, Y.-H.²

1) Korea Atomic Energy Research Institute, Taejon, Korea

2) Korea Advanced Institute of Science and Technology, Taejon, Korea

ABSTRACT : The seismic responses of a base isolated Pressurized Water Reactor(PWR) are investigated by using the mathematical model of which expresses the superstructure by a linear lumped mass-spring and the seismic isolator as an equivalent spring-damper. Time history analyses are performed by using the 1940 El Centro earthquake with linear amplification. In the analysis 5% structural damping is used in the superstructure. The four stiffness model types and varying isolator damping ratios from 2% to 100% are used to evaluate the effects of high damping rubber bearing on seismic response of the superstructure in base isolated system. The acceleration responses in base isolated PWR superstructure with high damping rubber bearings are much smaller than those in fixed base structure. However, when the damping ratio of the isolation system is above certain level, the peak acceleration at the superstructure starts to increase.

1. INTRODUCTION

The seismic isolation system used for the reduction of the seismic response of the structures is now promising device to be applied thru the world where large earthquakes are expected to occur. The seismic isolation systems are usually designed to lower the frequency of structure in the range of 0.5Hz to 0.7Hz, which prevents the structural damage from strong earthquakes having the high energy frequency range of 1.0 Hz to 10Hz. One of the seismic isolation system commonly used is a high damping laminated rubber bearing(HLRB). Since HLRB has a comparably large damping, both accelerations in superstructure and displacements between lower mat and upper base mat are remarkably reduced. However increasing damping ratio of the rubber bearings above certain level gives undesirable effects for the response of structural systems and components in superstructure[1]. The superstructural responses with varying the isolation damping are affected on the frequency contents of the excitation, the flexibility

and the damping of the superstructure[2].

Time history analyses for a typical PWR superstructure with a high damping rubber bearing isolation system were performed to understand the effects of various stiffness models for isolator and of flexibility for superstructure on seismic response and to determine damping ratio which gives the minimum seismic response in superstructures.

2. MATHEMATICAL MODEL

The model used in the analysis is shown in Fig.1. The isolated system considered in this paper consists of the isolator, base mat and the superstructure (containment vessel part and internal structure part). The computer program used in analysis is ABAQUS version 5.3[3]. The 2-dimensional beam element(type=B21) and mass element (type=MASS, type=ROTARYI) are used for the superstructure, and non-linear spring element (type=JOINTC) for the isolator.

In the model, the nodes from 1 to 10 represent the containment vessel part and the nodes from 11 to 17 represent internal structure part. The nodes 18, 7 and 11 represent the base mat, the polar crane support and the horizontal reactor vessel support respectively. The total weight of the superstructure is about 150,000 kips. The structural damping of the superstructure is assumed to be viscous damping with 5% damping ratio for all modes. It is converted into Rayleigh damping for the mathematical model.

Fig.2 shows the test results of the isolator which is scaled down 1/8 size. In modelling of the isolator which has severe hardening characteristics in large strain regions as shown in Fig.2, a simple equivalent viscous damping is applied for the damping model and the equivalent stiffnesses of the isolator are modelled with 4 types as shown in Table 1 and Fig.3.

Table 1. Spring models of the isolator

<u>Spring models</u>	<u>Equivalent stiffness values</u>
model 1 : linear spring 1	: $K_{eq} = 46.283 \times 10^6 \text{ lb}_f / \text{ft}$
model 2 : linear spring 2	: $K_{eq} = 70.639 \times 10^6 \text{ lb}_f / \text{ft}$
model 3 : bi-linear spring	: $K_1 = 46.283 \times 10^6 \text{ lb}_f / \text{ft}, K_2 = 174.130 \times 10^6 \text{ lb}_f / \text{ft}$
model 4 : multi-linear spring	: $K_1 = 46.283 \times 10^6 \text{ lb}_f / \text{ft}, K_2 = 53.426 \times 10^6 \text{ lb}_f / \text{ft}, K_3 = 112.14 \times 10^6 \text{ lb}_f / \text{ft}$

The K_{eq} 's of model 1 and 2 are determined by an extreme equivalent stiffness. In model 3, K_1 is same as the model 1 in the range of the displacement response from 0.0 ft to 2.23 ft, equivalent to strain 230% and K_2 acts in the range from 2.23 to 2.755 ft,

equivalent to the maximum strain 300%. In model 3, the stiffness is jumped from K1 to K2 which is about four times of K1. To reduce the transition effects between K1 and K2, another intermittent spring is considered in model 4.

3. EFFECTS OF STIFFNESS MODELING TYPES OF HLRB

The fundamental natural frequencies of the containment vessel and internal structure for fixed base[4] are 5.39 Hz and 15.73 Hz respectively, and for base isolated system are 5.94 Hz and 16.17 Hz respectively. The first frequency of the isolated system is 0.5 Hz. Fig.4 shows the first three mode shapes of the base isolated model.

The structural responses of the base isolated system having four different stiffness models of isolators but having identical viscous damping(12%) are analyzed and compared with those of fixed base structure. The isolated system is assumed to be subjected to horizontal ground motion of the linearly amplified 1940 El Centro earthquake up to the seven times. In the Fig.5 the zero period acceleration at the superstructure for the isolated system, of which represents rigid body motion, are remarkably reduced to 0.68g. It is noteworthy that the acceleration at the crane support for the fixed base system is 3.8g and that at reactor support is 2.4g respectively when it is subjected to five times El Centro earthquake. Figs.6 and 7 show the results of numerical simulation of the floor response spectrum at the polar crane support(node 7) and the reactor vessel support(node 11) of the superstructure, associated with the four stiffness models. The results essentially envisage that the responses depend on the flexibility of the superstructure and how one models the stiffness of the isolator.

From Figs.6 and 7, one can see that the models 3 and 4 which have large stiffness components in large strain ranges of the isolator, produce higher maximum peak accelerations by about 20% than models 1 and 2. This can be translated as that models 1 and 2 which have only one equivalent stiffness may not adequately represent the hardening phenomena of the rubber bearing at large strain. The resonant responses of the isolated system using the model 2 are slightly shifted to high frequency region and amplified around 0.7 Hz to 3 Hz to some extent, compared with other models. This is due to the fact that the equivalent stiffness for model 2 is higher by 1.5 times than the first stiffness for other models.

The model 3 having the highest stiffness value in high strain range has the higher value of the maximum peak acceleration in the range above 2.0 Hz than the Model 4 which has slowly increasing three different stiffnesses. The acceleration responses at the polar crane support of the containment vessel are slightly amplified around 6 Hz, and are also larger than those of the reactor vessel support of the internal structure because the

flexible structure can be excited larger than the stiff structure when subjected to an earthquake having lower frequency content excitation.

4. EFFECTS OF ISOLATOR DAMPING

In this paper, the effects of the isolator damping ratios on the superstructural responses are investigated by using the numerical simulations and the flexibility effects of the superstructure on the responses are also investigated.

The response locations of major concern are a polar crane support (node 7) in containment vessel part and the reactor vessel support (node 11) in internal structure part. Figs.8 and 9 show the results of the numerical simulations for the isolator damping ratio versus the floor response spectra at nodes 7 and 11 respectively. From these results one can see that the responses of the superstructure are decreased as increasing the damping ratio of the isolator but increasing the isolator damping beyond some level enlarges the maximum peak values of the superstructural accelerations. Figs.10 and 11 show the results of the numerically simulated damping effects. Fig.10 essentially demonstrates that maximum peak acceleration of both the flexible structure(polar crane) and stiff structure(reactor support) does not depend linearly on damping; their minimums occur at 40% and 65% respectively. An increase of flexibility of superstructure tends to lower the damping ratio to obtain the minimum peak acceleration of the superstructure. In the meanwhile, as illustrated in Fig. 11, the relative displacements between lower mat and upper base mat decrease monotonously as increase of damping ratio of isolator.

5. CONCLUSIONS

Based on this study, the followings are concluded

The acceleration responses in base isolated PWR superstructure subjected to linearly amplified 1940 El Centro earthquake are much smaller than those in fixed base superstructure.

In the higher strain region where stiffness behaves non-linearly, the acceleration responses modelled by one equivalent stiffness are smaller than those in nonlinear spring model, and the higher stiffness spring model of isolator exhibits larger peak acceleration response at superstructure in the frequency range above 2.0 Hz, when subjected to linearly amplified 1940 El Centro earthquake.

Peak accelerations at the certain level of the base isolated superstructure decrease

sharply as increase of damping ratio of the isolator up to 15%, and minimum peak acceleration can be obtained by 40 % damping ratio of the isolator for flexible containment vessel and by 65 % for stiff internal structure. However as increase of damping ratio of the isolator above this value in each structure, peak accelerations at both structures increase, and peak accelerations at flexible structure increase more than those at stiff structure. This means that the secondary components and systems at flexible structure may have more unfavorable effects than those at stiff structure. The relative displacements between lower mat and upper base mat decrease monotonously as increase of damping ratio of isolator.

REFERENCES

1. Tsai, H.C. and Kelly, J.M. 1993. Seismic response of heavily damped base isolation systems: Earthquake engineering and structural dynamics. Vol.22: 633-645.
2. Inaudi, J.A. and Kelly, J.M. 1993. Optimum damping in linear isolator system: Earthquake engineering and structural dynamics. Vol.22: 583-598.
3. ABAQUS Version 5.3, Standard user's manual I,II.
4. Yun, C.H. et al. 1994. A study of major seismic safety issues for nuclear power plants(1): Report No. KINS/GR-067 (in Korea).

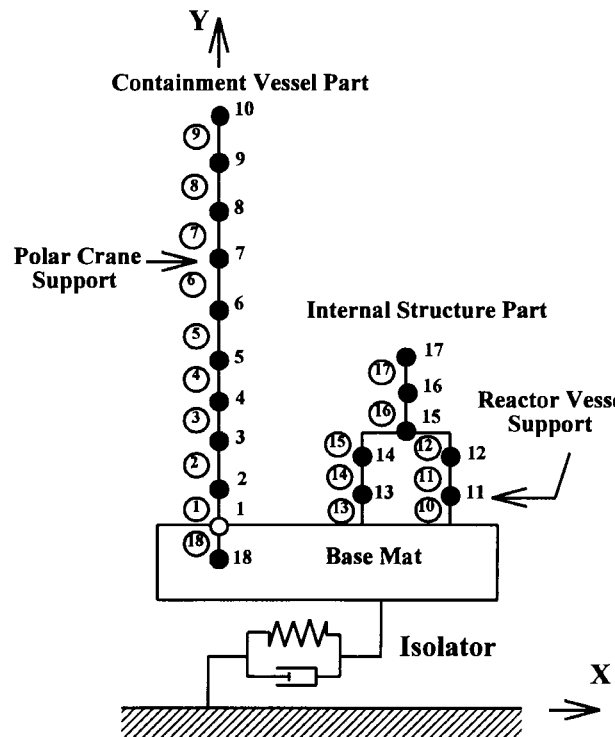


Fig. 1. Analysis model of base isolated system

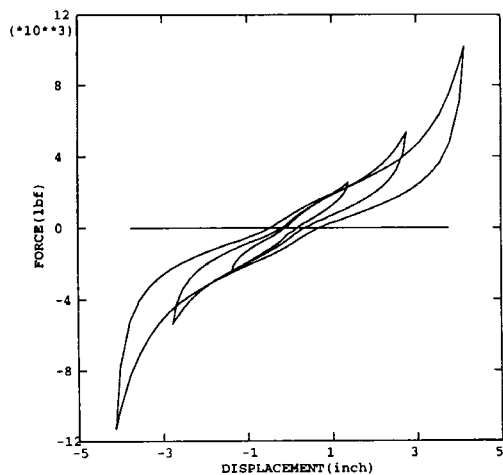


Fig. 2. Hysteretic curve of the 1/8 scale rubber bearing test

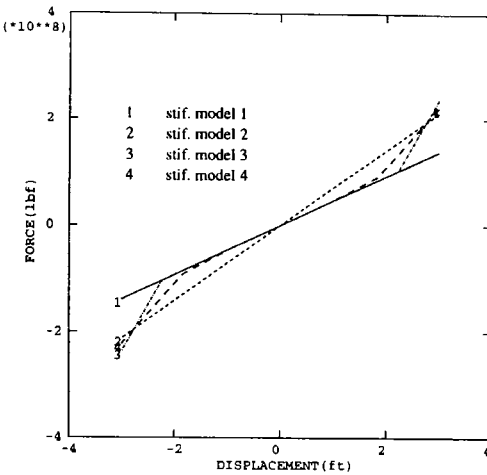


Fig. 3. Horizontal equivalent stiffness models of isolator

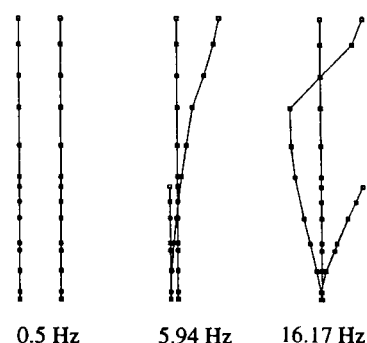


Fig. 4. Mode shapes of base isolated superstructure

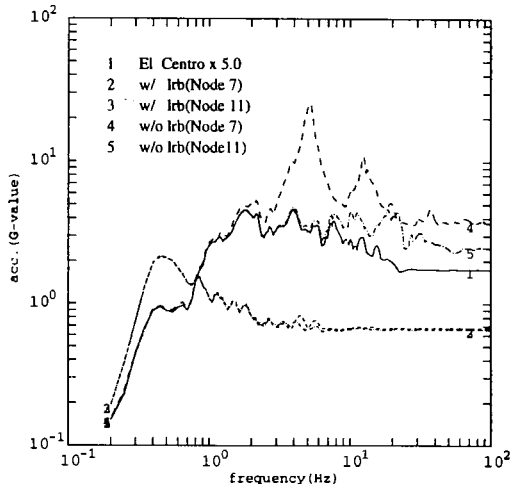


Fig. 5. Acceleration response spectra of base isolated and fixed base superstructure

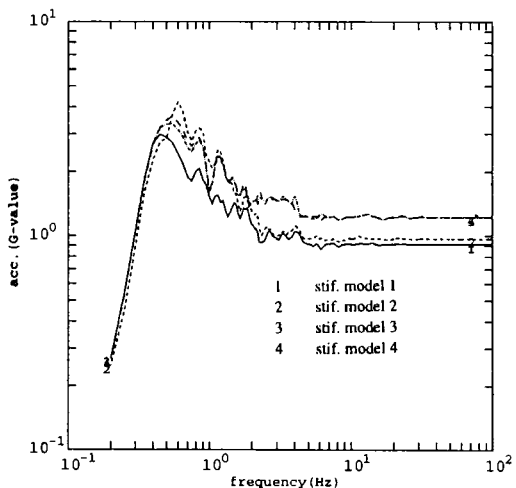


Fig. 6. Effects of equivalent stiffness model at polar crane support (node 7)

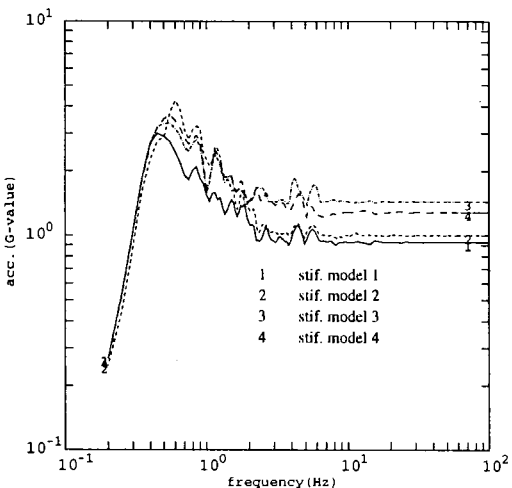


Fig. 7. Effects of equivalent stiffness model at reactor vessel support (node 11)

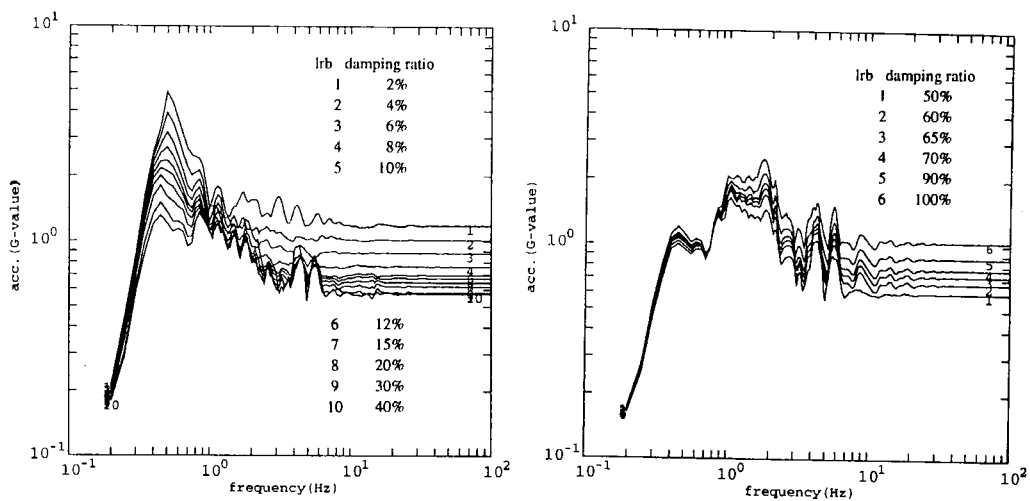


Fig. 8. Effects of isolator damping at polar crane support (node 7)

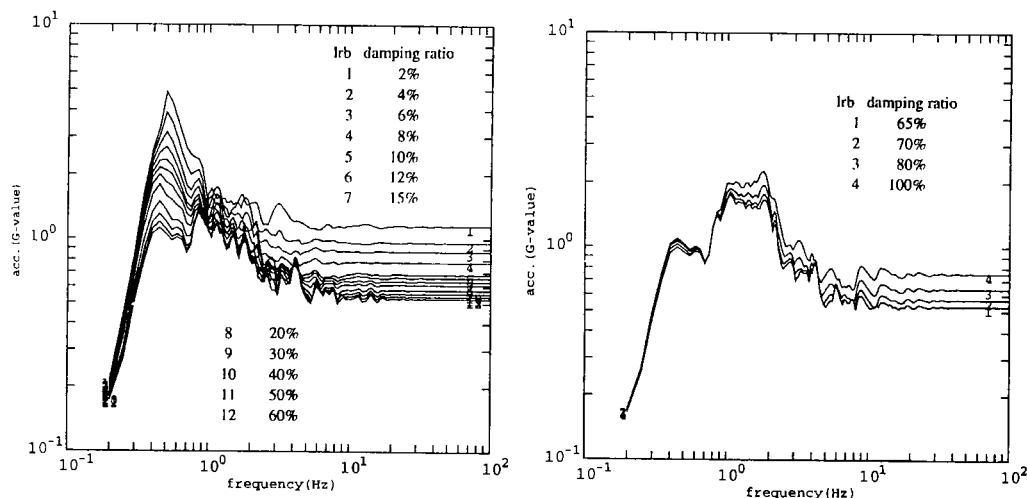


Fig. 9. Effects of isolator damping at reactor vessel support (node 11)

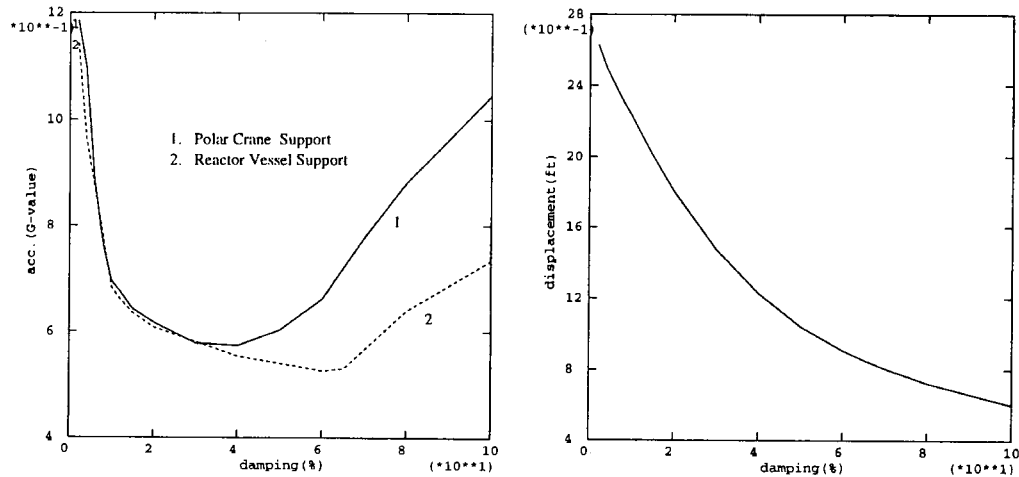


Fig. 10. Maximum peak accelerations vs. isolator damping

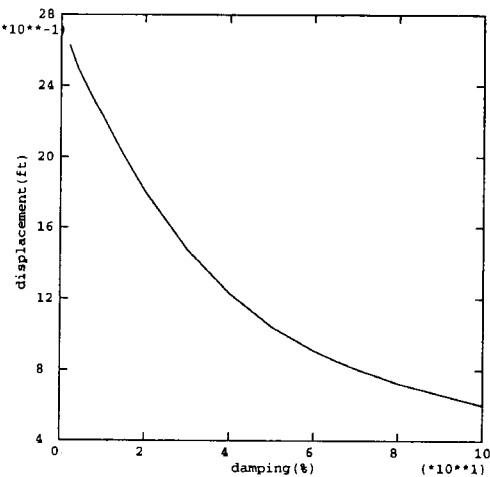


Fig. 11. Maximum relative displacements vs. isolator damping

